We are IntechOpen, the world's leading publisher of Open Access books Built by scientists, for scientists

4,800
Open access books available

122,000
International authors and editors

135M
Downloads

Our authors are among the

154
Countries delivered to

TOP 1%
most cited scientists

12.2%
Contributors from top 500 universities

CLARIVATE ANALYTICS BOOK CITATION INDEX INDEXED

WEB OF SCIENCE™

Selection of our books indexed in the Book Citation Index in Web of Science™ Core Collection (BKCI)

Interested in publishing with us?
Contact book.department@intechopen.com

Numbers displayed above are based on latest data collected.
For more information visit www.intechopen.com

8

Zeolite nanocrystals - synthesis and applications

Teruoki Tago and Takao Masuda
Division of Chemical Process Engineering, Faculty of Engineering, Hokkaido University
N13W8, Kita-Ku Sapporo, Hokkaido, 060-8628, Japan

1. Introduction

Zeolites, crystalline aluminosilicate materials, possess 3-dimensionaly connected framework structures constructed from corner-sharing TO_4 tetrahedra, where T is any tetrahedrally-coordinated cation such as Si and Al. These framework structures are composed of n-rings, where n is the number of T-atoms in the ring (e.g. 4-, 5-, and 6-rings), and large pore openings of 8-, 10-, and 12-rings are framed by these small rings. Figure 1 shows the pore sizes and framework structures of typical zeolites. The sizes of the intracrystalline pores and nanospaces, depending on the type of zeolite providing the framework, are close to the molecular diameters of lighter hydrocarbons. Moreover, strong acid sites exist on the nanopore surfaces, enabling the zeolites to be used as shape-selective catalysts in industrial applications such as fluid catalytic cracking of heavy oil, isomerization of xylene and synthesis of ethyl-benzene. However, compared to the sizes of micropores exhibiting a molecular-sieving effect, the crystal sizes of zeolites are very large, approximately 1–3 μm. When the zeolite is used as a shape-selective catalyst, the diffusion rates of reactant molecules within the zeolite crystals are lower than the intrinsic reaction rates. This resistance to mass transfer limits the reaction rates and low selectivity of intermediates. Moreover, since effective active sites (acid sites) for catalytic reactions are distributed on the internal surfaces of the main channels and the external surfaces of the crystal, the pore mouths are easily plugged due to coke deposition, leading to short lifetimes for the catalysts.

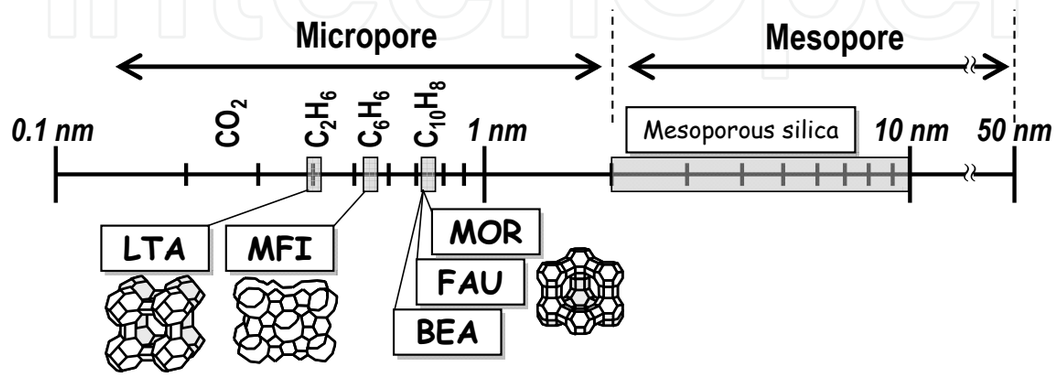

Fig. 1. Zeolite structure, pore size and molecular diameter of hydrocarbons.

Faster mass transfer is required to avoid these serious problems, and two primary strategies have been proposed; one is the formation of meso-pores within zeolite crystals (Groen et al., 20004a, 2004b; Ogura et al., 2001), and the other is the preparation of nano-crystalline zeolites (Tsapatsis et al., 1996; Mintova et al., 1999, 2002, 2006; Ravishankar et al., 1998; Grieken et al., 2000; Hincapie et al., 2004; Song et al., 2005; Larlus et al., 2006; Morales-Pacheco et al., 2007; Kumar et al., 2007).
In nano-crystalline zeolites, the diffusion length for reactant hydrocarbons, assignable to the crystal size, decreases, and the external surface area of the crystal increases as the crystal size decreases. The increase in external surface area and the decrease in diffusion resistance are effective for improving catalytic activity in gas-solid and liquid-solid heterogeneous catalytic reactions. Because of these favorable properties of nano-crystalline zeolites for catalytic reactions, the preparation methods for several types of zeolite nanocrystals have been reported and reviewed (Tosheva & Valtchev, 2005; Larsen, 2007).
In this chapter, a method for preparing nano-crystalline MFI and MOR zeolites in a solution consisting of a surfactant, organic solvent, and water is introduced (denoted as the emulsion method hereafter). Nano-crystalline zeolite is expected to be a promising material for increasing the outer surface area as well as decreasing the diffusion resistance of the organic reactant within the micropores, thereby improving the catalytic activity and lifetime.

2. Synthesis of nano-crystalline zeolites in water/surfactant/organic solvent

Usually, zeolites are prepared in an alkaline water solution containing Si and Al sources, and alkaline metal ions (sodium or potassium). In the synthesis of some types of zeolite, an organic structure directing agent (OSDA), such as an ammonium alkyl cation, is also necessary to form the zeolite framework. The water solutions containing these inorganics and OSDA are poured into a Teflon-sealed stainless steel bottle and heated to a desirable temperature.
In some types of zeolites (e.g. MFI and MOR), crystal nucleation occurs first, followed by the growth of the zeolite, with the nucleation simultaneously continuing to occur during the growth stage. One method to prepare nano-crystalline zeolite is the stoppage of the hydrothermal treatment when the nucleation occurs. However, because unreacted Si and Al species still remain in the solution, an amorphous phase tends to form on the surface of the zeolite crystals. Another method is increasing the nucleation rate by increasing the concentrations of the Si and Al sources. With increasing nucleation rate, the crystal size of the zeolite decreases. However, the zeolite thus obtained has a broad size distribution due to simultaneous nucleation and crystal growth during the hydrothermal treatment. Accordingly, in order to obtain nano-crystalline zeolites, it is important to separate the nucleation and growth stages. Recently, there has been growing interest in the synthesis of nano-crystalline zeolites with the addition of surfactants, including water/surfactant/organic mixture (Kuechl et al., 2010; Naik et al., 2002; Lee et al., 2005; Tago et al., 2004, 2009a, 2009b) (emulsion method), with research focused on size and morphology control, because these parameters affect the performance in applications, such as separation and catalytic reactions. Because surfactant molecules that have hydrophobic and hydrophilic organic groups in the molecules are adsorbed on a solid surface in a solvent, the interface energy difference between the solid surface and solvent can be reduced, leading to

enhancement of nucleation of metal and/or metal oxide nano-particles. In the emulsion method, the surfactant adsorption effect is applied to prepare nano-crystalline zeolites.
In general, there are four types of surfactants, anionic, cationic, nonionic, and bipolar surfactants. A nonionic surfactants; Polyoxyethylene(15)oleylether (O-15), polyoxyethylene(15)nonylphenylether (N-15), and poly(oxyethylene)(15)cethylether (C-15), and ionic surfactants, sodium bis(2-ethylhexyl) sulfosuccinate (AOT) and cetyltrimethyl ammonium bromide (CTAB), are employed. (Figure 2) Cyclohexane or 1-hexanol is used as an organic solvent.

nonionic surfactant

polyoxyethylene(15)nonylphenylether :(NP-15)

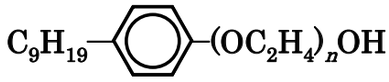

Polyoxyethylene(15)oleylether : (O-15)

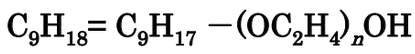

poly(oxyethylene)(15)cethylether : (C-15)

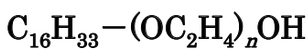

ionic surfactant

cetyltrimethyl ammonium bromide : (CTAB)

sodium bis(2-ethylhexyl) sulfosuccinate : (AOT)

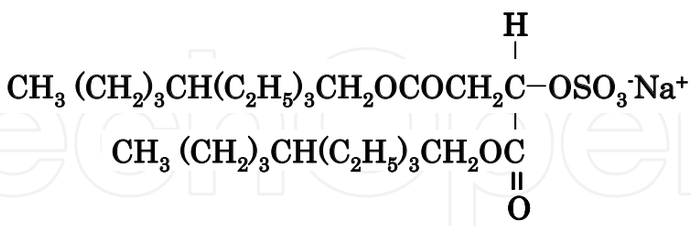

Fig. 2. Typical molecular structures of surfactants.

In the emulsion method, two solutions are prepared, one is a water solution containing Si and Al sources obtained by hydrolyzing metal alkoxide with a dilute OSDA/water solution, and the other is a surfactant/organic solvent. The concentrations of the Si and Al sources in the water solution and the molar ratio of Si to the OSDA as well as types of the OSDA are very important factors in preparing zeolite crystals. In the case of MFI, tetrapropylammoniumhydroxide (TPAOH) is used as an OSDA, and tetraethylammoniumhydroxide (TEAOH) is used for the preparation of MOR zeolite.

Moreover, two additional parameters, the concentration of surfactant in the organic solvent and the molar ratio of water to surfactant, are important in the emulsion method. These parameters affect the morphology and crystal sizes.

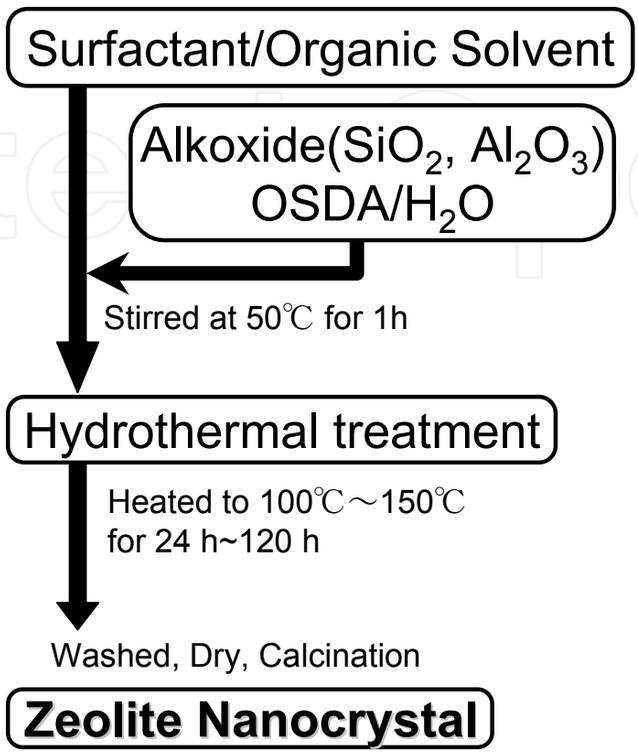

Fig. 3. Preparation procedure for nano-crystalline zeolite by the emulsion method.

The water solution thus obtained is added to the surfactant-organic solvent, and the mixture is magnetically stirred at 323 K for 1 h. The water/surfactant/organic solvent mixture is then placed in a Teflon-sealed stainless steel bottle, heated to 373 ~ 423 K, and held at the desired temperature for 12 ~ 120 h with stirring to yield zeolite nanocrystals. The precipitate thus obtained is centrifuged, thoroughly washed with propanol, dried at 100 °C overnight, and calcined under an air flow at 500 °C to remove the surfactant and the OSDA molecules. After the air calcination, the weight of the sample is measured to calculate the zeolite yield (Figure 3).

2.1 Effect of ionicity of surfactant on preparation of MFI zeolite nanocrystals

The morphologies of the silicalite-1 (MFI zeolite) nanocrystals prepared using various surfactants were investigated under conditions of TOES concentration of 0.63 or 2.73 mol/L, hydrothermal temperature of 140 or 100 °C and concentration of surfactant in organic solvent (solution B) of 0.50 mol/L. Figures 4 and 5 show X-ray diffraction (XRD) patterns and FE-SEM images of the obtained samples, respectively.

In the XRD pattern for the sample prepared in the AOT/cyclohexane solution, peaks corresponding to sodium sulfate rather than silicalite-1 are seen. Moreover, the sample showed an irregular morphology. In this case, the TPA-OH molecules cannot act as an OSDA in the synthetic solution. This result is ascribed to the fact that the surfactant of AOT and the OSDA of TPA-OH have opposite ionic charges.

When using CTAB/1-hexanol, the silicalite-1 crystals, which are approximately 1.0 μm in size, are embedded in the amorphous SiO_2 as seen from SEM observations. The coexistence of silicalite-1 crystals and amorphous SiO_2 is revealed by the X-ray diffraction analysis. Since the pH of the synthetic solution is alkaline, the surface of the SiO_2 produced by hydrolysis of TEOS has a negative charge. Accordingly, it is considered that CTAB and TPA-OH are independently adsorbed on the surface of SiO_2 because of their cationic ionicity. Therefore, the SiO_2 species that adsorb TPA-OH and CTAB change into silicalite-1 crystals and amorphous SiO_2, respectively.

In the case of the nonionic surfactants, C-15, NP-15 and O-15 (the nonionic surfactant/cyclohexane system), the XRD patterns of the samples showed peaks corresponding to pentasile-type zeolite (the reference silicalite-1), and mono-dispersed silicalite-1 nano-crystals were obtained, as seen from SEM observations. In contrast, the silicalite-1 crystal prepared in water (without a surfactant) shows a heterogeneous structure with smaller crystals (diameter of approximately 30 nm) on a larger one (approximately 120 nm), indicating that nucleation, crystallization and crystal growth occurred simultaneously. These results indicate that the ionicity of the hydrophilic groups in the surfactant molecules plays an important role in the formation and crystallization processes of the silicalite-1 nanocrystals. Since the aggregation of the silicalite-1 nuclei are inhibited by the adsorbed surfactants on the surface during hydrothermal treatment, mono-dispersed nanocrystals can be prepared.

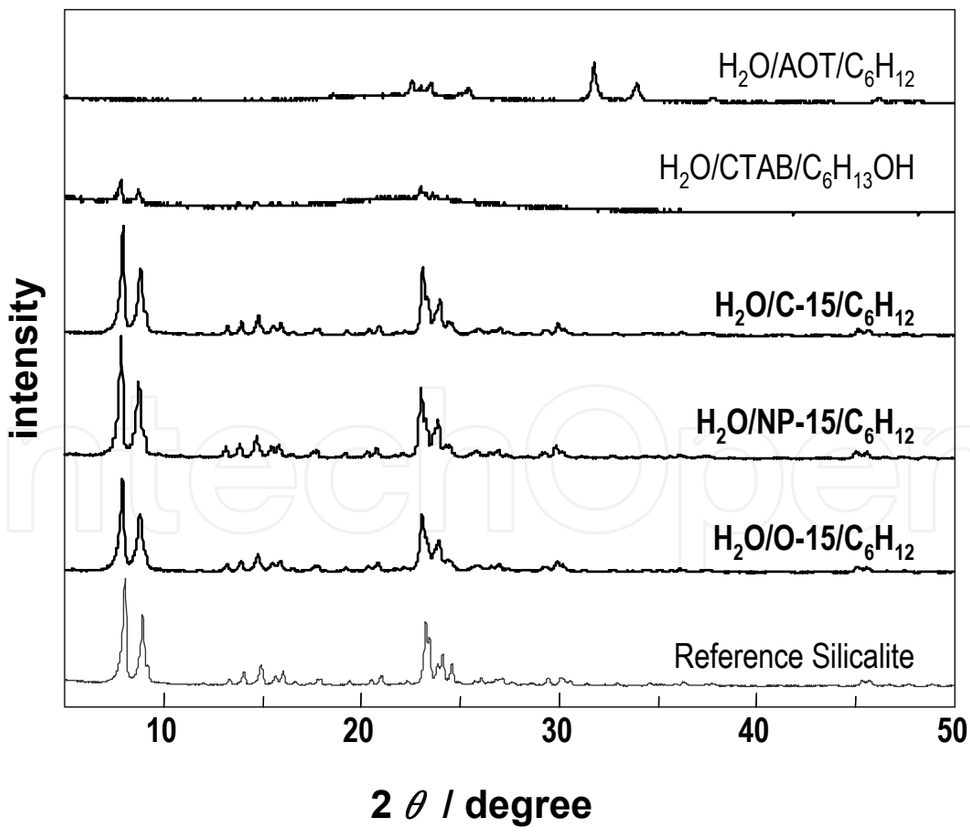

Fig. 4. X-ray diffraction patterns of samples prepared in water/surfactant/organic solvent. Effects of ionicity of the surfactant on crystallinity of MFI zeolite (Silicalite-1).

Nano-crystalline zeolite has a high external surface area, which is very important for use as heterogeneous catalysts and as seed crystals. To evaluate the crystallinity of the nanocrystals, X-ray diffraction patterns and Raman spectroscopy can be used. The former is based on elastic scattering of X-rays from structures that have long range order (zeolite crystal structure, types of zeolite), and the latter method can elucidate middle-range order (types of Si-O rings). Accordingly, the Raman spectra measurements are useful to evaluate the zeolite crystallinity in detail (Dutta et al., 1991; Li et al., 2000, 2001). Figure 6 shows the Raman spectrum of the silicalite-1 nanocrystals. The peaks in the range of 300 – 650 cm^{-1} are indicative of the type of silicon-oxygen rings present in the structure of zeolite. The spectrum also shows peaks around 380, 430 and 470 cm^{-1}, which correspond to the five-, six- and four-member rings, respectively. These peaks are in good agreement with the peaks of the reference silicalite-1 prepared in water. In the structure of the MFI-type zeolite, continuous chains of five-member rings are connected by the four- and six-member rings. These results indicated that the surfaces of the nanocrystals with a diameter of approximately 120 and 80 nm are also well-crystallized without amorphous SiO_2.

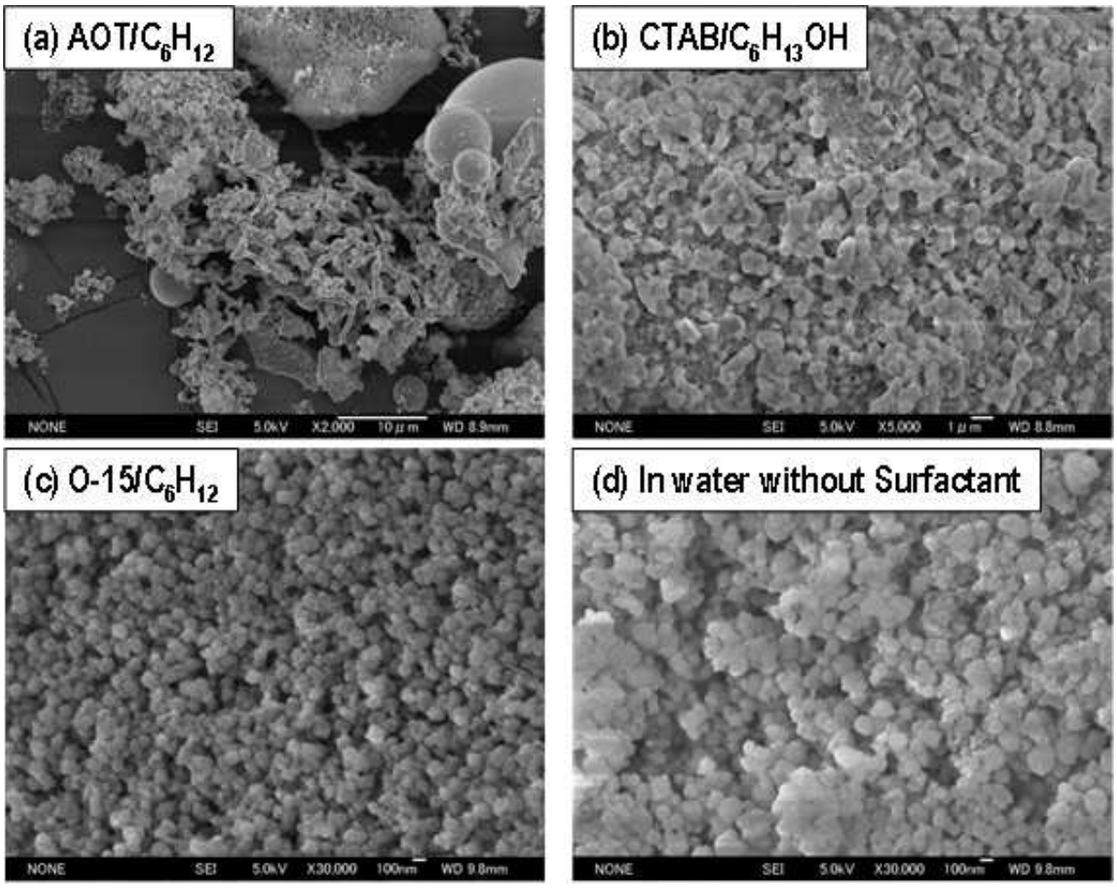

Fig. 5. FE-SEM micrographs of samples prepared in water/surfactant/organic solvent. Effects of ionicity of the surfactant on crystallinity of MFI zeolite (Silicalite-1).

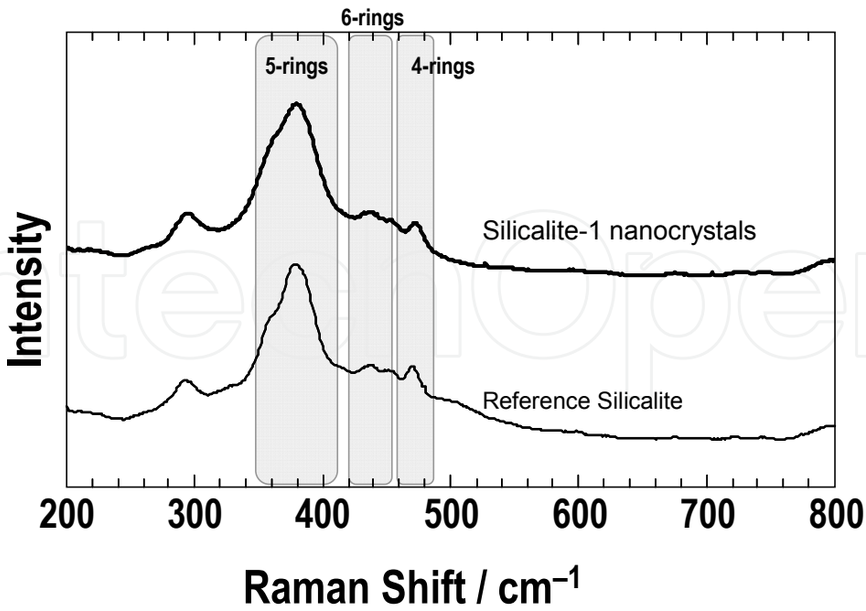

Fig. 6. Raman spectrum of the nanocrystals.

2.2 Preparation of MOR zeolite by the emulsion method

In the preparation of MFI zeolite nanocrystals by the emulsion method, since the non-ionic surfactant is revealed to be the appropriate surfactant to prepare nano-crystalline zeolite, this method is applied to prepare MOR zeolite nanocrystals as well. First, the effects of the hydrothermal time on the crystallinity of MOR zeolite prepared in water/O-15/cyclohexane are examined. The concentrations of Si in a water solution and a surfactant in cyclohexane are 0.75 and 0.5 mol/L, respectively, and the hydrothermal temperature is 423 K. Figure 7 shows the X-ray diffraction patterns of MOR zeolite prepared using the emulsion method with different hydrothermal times. The X-ray diffraction patterns of samples prepared in the water solution without a surfactant (conventional method) are also shown in the figure for comparison.

The samples prepared in the water solution show a broad halo pattern of SiO_2 at hydrothermal times of 72 and 96 h, and show peaks corresponding to MOR zeolite as well as BEA zeolite (beta-type zeolite) at 120 h. In contrast, as compared to the sample prepared in the water solution, though an amorphous pattern is observed from the sample prepared at a hydrothermal time of 72 h, the samples at hydrothermal times of 96 and 120 h show peaks corresponding to MOR zeolite. Moreover, peaks ascribable to other types of zeolite, e.g. MFI and BEA, cannot be detected. Because hydrolysis of the Si (tetraethylorthosilicate) and Al (aluminum-tri-isopropoxide) sources should be completed during the preparation of water solution containing Si, Al, and the OSDA molecules (TEA-OH), the appearance of the diffraction peaks corresponding to MOR zeolite after 96 h indicates that the MOR zeolite precursors are prepared in the solution until approximately 72 h, followed by nucleation and crystal growth of MOR zeolite. Accordingly, MOR and MFI zeolites can be prepared in water/surfactant/organic solvent. Sizes control by the emulsion method is next examined.

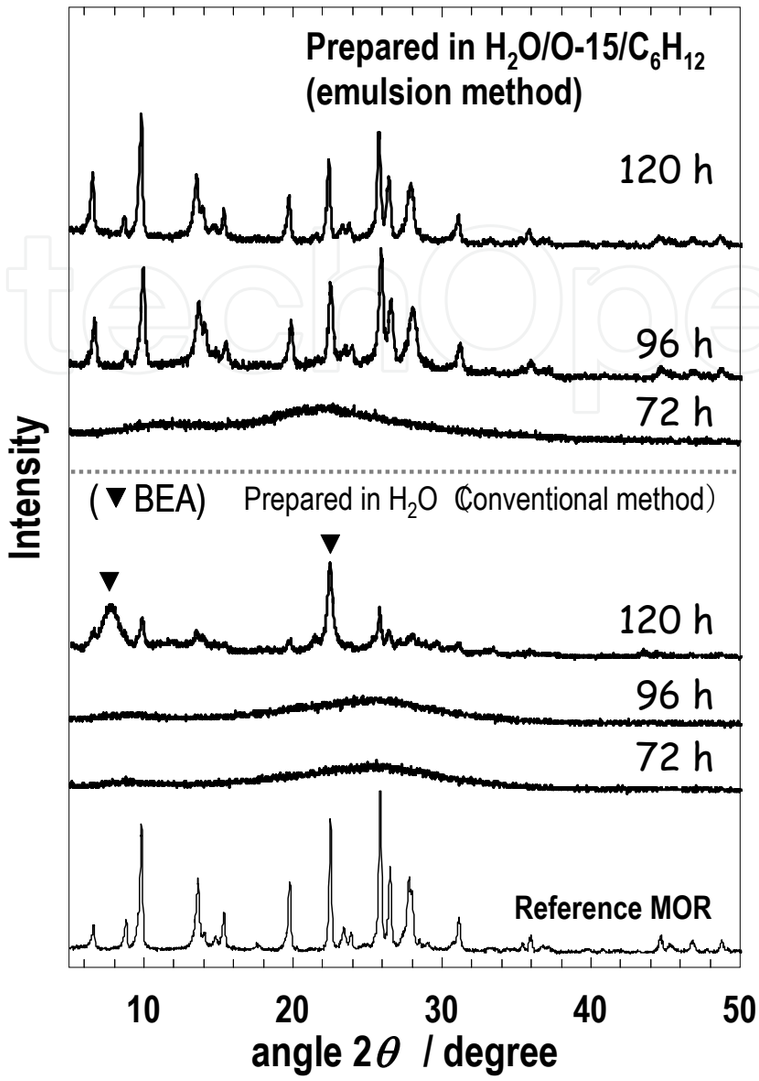

Fig. 7. X-ray diffraction patterns of MOR zeolite prepared in the emulsion method with different hydrothermal times.

2.3 Crystal size control

In a catalytic reaction using a zeolite, the reaction proceeds on acid sites located on the outer surface of the crystal as well as the inside pore surface. The crystalline zeolite affects the outer surface area and the diffusion length, assignable to the crystal size, for reactant hydrocarbons within the crystal. Accordingly, it is very important to develop preparation methods for zeolite nanocrystals with different crystal sizes.

In the emulsion method, it is considered that non-ionic surfactants adsorbed on the surfaces of zeolite precursors induce the formation of zeolite nuclei, enhancing the nucleation of zeolite. Moreover, the surfactant concentration in the solution can be easily changed. Accordingly, the effects of varying surfactant concentration [O-15] on the morphology of MOR zeolite were examined. Figure 8 shows FE-SEM images of the obtained samples. The Si/Al ratio is 12.5. The surfactant concentrations were changed in the range from 0.5 to 0.75

mol/L. Interestingly, the crystal size and morphology depended on the surfactant concentration, regardless of the same concentrations of the Si and Al sources, and template in the water solution. MOR zeolite nanocrystals with an average size of approximately 80 nm were obtained at a surfactant concentration of 0.5 mol/L. As the concentration increased to 0.65 mol/L, growth of MOR zeolite with column-like morphology is observed, and the crystal size reached ~1.0 μm at 0.75 mol/L. Figure 9 shows NH_3–TPD profiles and N_2 adsorption–desorption isotherms of the obtained samples, respectively, at surfactant concentrations of 0.5 and 0.75 mol/L. The NH_3–TPD profiles of these sample shows NH_3 desorption peaks above 600 K, ascribable to desorption of NH_3 from strong acid sites of MOR zeolites. Moreover, these MOR zeolites show almost the same peak area. The MOR zeolites also show almost the same N_2 adsorption–desorption isotherms, indicating that these zeolites exhibit almost the same surface area. Accordingly, these MOR zeolites possess almost the same number of acid sites, regardless of the crystal morphology.

As discussed above, it is revealed that the surfactant in the synthetic solution induces the nucleation and crystallization of zeolite as compared to the conventional preparation method (without a surfactant). Moreover, the surfactant concentrations in the solution were found to influence crystal growth. The crystal morphology changed from the nano–crystalline to large columnar crystals with increasing surfactant concentration.

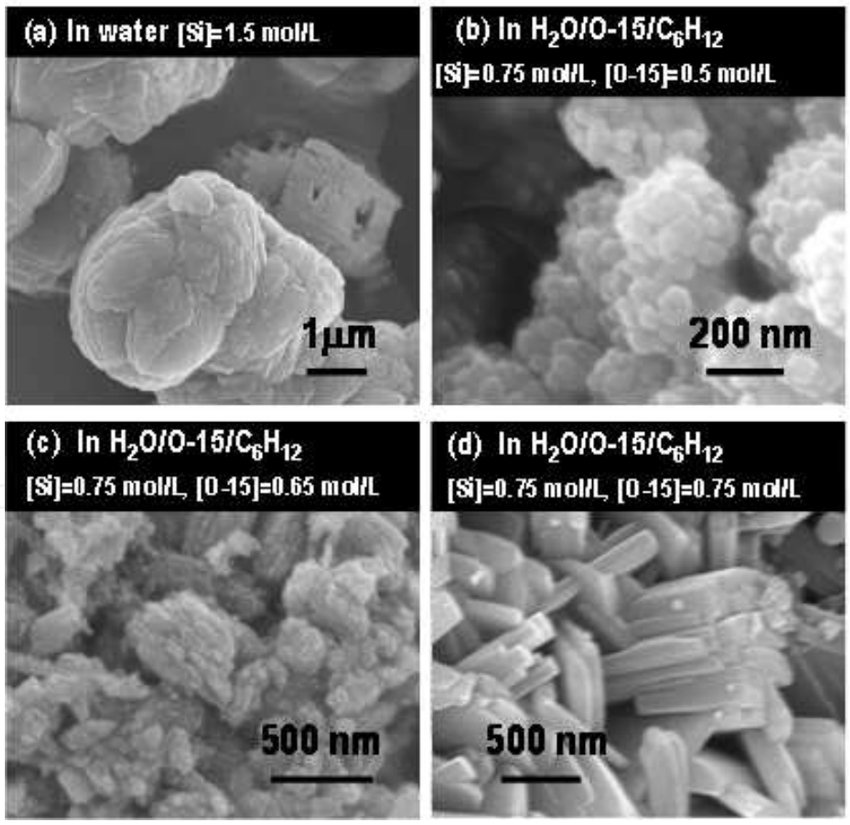

Fig. 8. FE-SEM micrographs of MOR zeolite with different crystal sizes. (Tago *et al.*, (2009b))

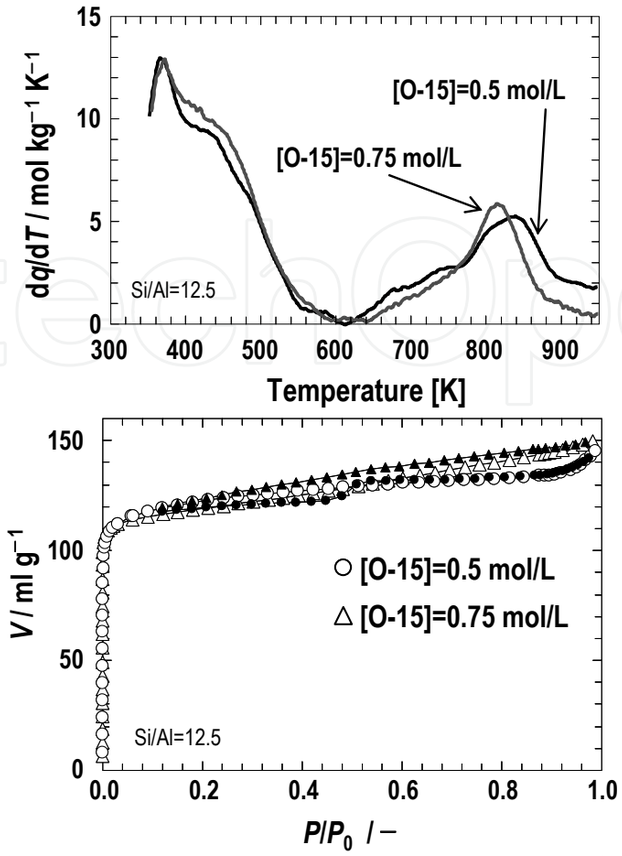

Fig. 9. NH_3–TPD profiles and N_2 adsorption–desorption isotherms of the MOR zeolite with different crystal sizes. (Tago *et al.*, (2009b))

2.4 Mechanism

In order to consider the mechanism of zeolite nanocrystals formation in water/surfactant/organic solvent, it is necessary to investigate the relationship between the ionicity of the surfactant and the template molecule, and the ionic charges of the surface of SiO_2 and/or zeolite precursor in detail.

In the method, the cyclohexane used as the organic solvent contributes to stabilization of the hydrophobic group of the surfactant. The effects of the ionicity of the hydrophilic group of the surfactant on the morphology and crystallinity of the obtained silicalite-1 zeolite nanocrystals are described above.

In an anionic surfactant (e.g. sodium bis(2-ethylhexyl) sulfosuccinate, AOT), because the surfactant of AOT has opposite ionic charges to the OSDA molecules, the OSDA cannot act as a structure-determining agent in the synthetic solution. Accordingly, in the relationship between the ionicity of the surfactant and OSDA molecules, a surfactant without electrostatic affinity to the OSDA molecules is needed for the preparation of zeolite crystals. In a cationic surfactant (e.g. cetyltrimethyl ammonium bromide, CTA-Br), the molecular structure is similar to that of the OSDA. Moreover, since the surface charge of the SiO_2 and/or zeolite precursor is negative, the surfactant molecules of CTA^+ with cationic hydrophilic group can be adsorbed on the surface, followed by the formation of amorphous SiO_2. In contrast, in the case of nonionic surfactants, MOR as well as MFI zeolite nanocrystals can be obtained.

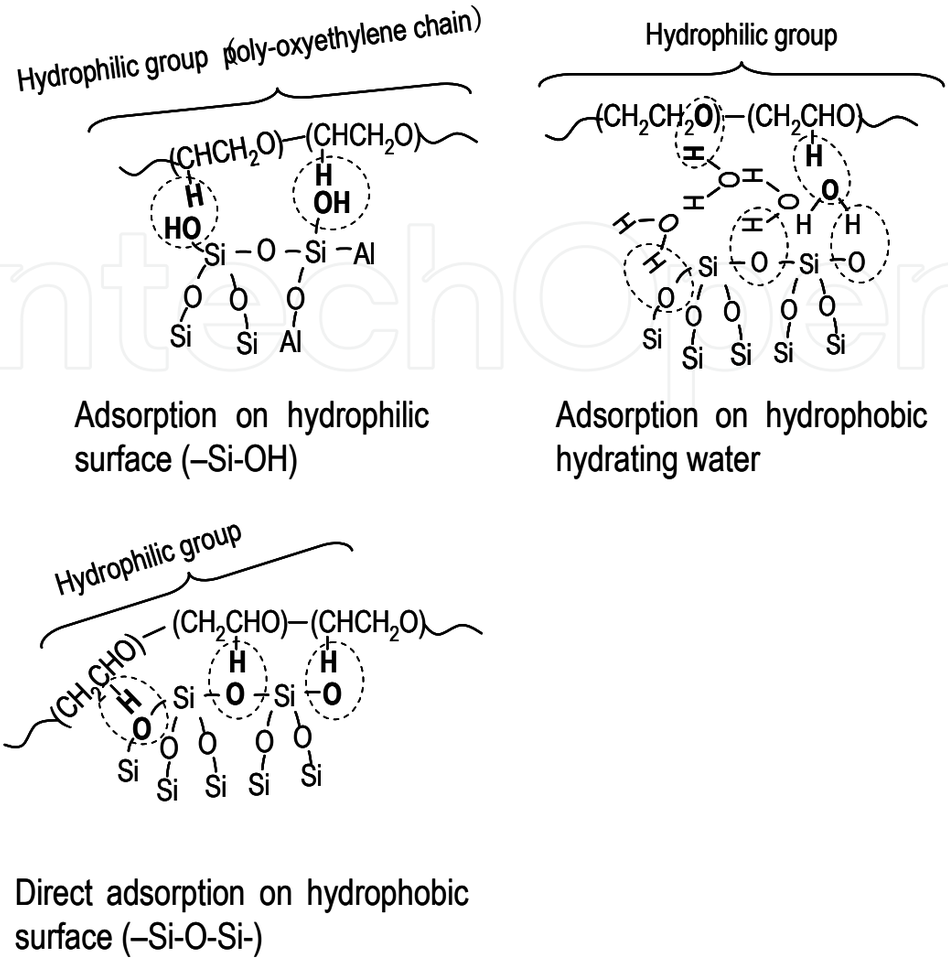

Fig. 10. A schematic showing the possible relationship between the surfactant and the zeolite surface. (Tago *et al.*, (2009b))

A schematic figure showing the possible relationship between the surfactant and the zeolite surface is shown in Fig. 10. The hydrophilic group of the surfactant O-15 is composed of poly-oxyethylene chains, making it a non-ionic surfactant. The surface of the zeolite precursor and crystal is composed of a hydrophobic surface (-Si-O-Si-) and hydrophilic silanol groups (-O-Si-OH). The hydrophilic groups of the surfactant can be adsorbed on the hydrophilic silanol groups, leading to stabilization of the silanol groups. On the hydrophobic surface, hydrophobic hydration occurs in the conventional preparation method without a surfactant (Burkett & Davis, 1994, 1995; De Moor, 1999a, 1999b). It is considered that the hydrophilic groups of the surfactant are adsorbed onto the water molecules hydrophobically-hydrated on the zeolite surface. Moreover, because the hydrophilic property of the poly-oxyethylene chains in the surfactant is much smaller than that in water, it is considered that the hydrophilic poly-oxyethylene chains can be directly adsorbed onto the zeolite surface due to their higher affinity to the zeolite surface than water molecules. These adsorbed surfactants can contribute to the stabilization of the surface of zeolite precursor and crystals, which will influence the nucleation rate of zeolite, so that the MOR zeolite nanocrystals can be obtained.

Three-dimensional cylindrical networks of the micellar structure composed of water and surfactant molecules likely exist in water/O-15/cyclohexane solvent, wherein silica-based cylindrical (Matsune et al., 2006) and spherical (Tago et al., 2002, 2003; Takenaka et al., 2007) materials including metal and/or metal-oxide nano-particles are obtained at 323 K. These networks lead to an increase in the viscosity of the solvent. Though the reaction temperature of 323 K is different from the hydrothermal temperature, the viscosity of the zeolite synthetic solution is thought to be high. It is considered that the viscosity of the solvent affected the nucleation rate and diffusion of silicate species. However, since the yields of zeolite are above 80%, the diffusion of silicate species in the solution is likely not a rate-limiting step to form zeolite nanocrystals, and thus the viscosity affects the nucleation rate. Moreover, as the surfactant concentration is increased, the excessive stabilization of the precursors and the high viscosity of the solution lead to a decrease in the nucleation rate of zeolite. Since the growth rate of the crystal is much higher than the nucleation rate, crystalline growth of the MOR zeolite is dominant at high surfactant concentrations, so that column-like crystals with a large size are obtained. Accordingly, the surfactant can play an important role in the nucleation and crystal growth of the MFI and MOR zeolite prepared in the water/surfactant/organic solvent (emulsion method), and the crystal size and morphology can be controlled by the surfactant concentration.

3. Applications of nanocrystals

3.1 Heterogeneous catalytic reaction over zeolite nanocrystals

The acid sites in zeolites are located on the external and internal surfaces. In nano-crystalline zeolite, the external surface area of the crystal increases and the diffusion length for reactant hydrocarbons, assignable to the crystal size, decreases as the crystal size decreases. Due to these favorable properties, nano-crystalline zeolites have been used as heterogeneous catalysts.

Zeolites exhibit a molecular sieving effect for lighter hydrocarbons, hence, the hydrocarbon molecules with sizes larger than the pore mouth size are mainly adsorbed on the external surface. Accordingly, an increase in the external surface area is effective for increasing catalytic activity. Song *et al.* (2004a, 2004b) reported the preparation of nano-crystalline MFI zeolites and they evaluated the effects of crystal size on external surface area and adsorption properties of toluene on the zeolite. Since the molecular size of toluene is almost the same as the pore mouth size in MFI zeolite, the external surface area, which is a function of the crystal size, affects the adsorption capacity for toluene. Zeolites with crystal sizes less than 100 nm have a higher adsorption capacity for toluene. Botella *et al.* (2007) have reported the Beckmann rearrangement reaction over nanosized BEA zeolite where the reactions mainly proceed on the external surface of zeolite. Serrano *et al.* (2005) have reported catalytic cracking of polyolefins over nano-crystalline MFI zeolite. Because the molecular size of polyolefins is larger than the pore size, cracking of polyolefins mainly occurs over the acid sites on the external surface, while the formation of lighter olefins proceeds on the internal pore surface. Jia *et al.* (2010) have reported dehydration of glycerol to produce acrolein over nano-sized MFI zeolite. Since the hydrophilic glycerol molecules are strongly adsorbed on the external surface of the zeolite, nano-crystalline MFI zeolite is effective for this reaction due to the high surface area. In these reports listed above, the increase in the external surface area of the zeolite nanocrystal is important to improve the catalytic activity and lifetime.

In contrast, Sakthivel *et al.* (2009) have reported the isomerization/cracking of hexane over nano-sized BEA zeolite. Since the molecular size of hexane is smaller than the pore size of MFI zeolite, the cracking reaction proceeds mainly on the acid sites located inside pores. Moreover, the small crystal size of BEA zeolite leads to low diffusion resistance of the reactant hexane and the products. Serrano *et al.* (2010) have reported epoxide rearrangement reactions over MFI zeolite, where the high external surface area and low diffusion resistance within the micropores due to the small zeolite crystal size enhance the rearrangement reaction without diffusion restriction of the epoxide molecules.
MFI zeolites are effective catalysts to synthesize lighter olefins by the methanol-to-olefin (MTO) reaction and acetone conversion to olefin. In these olefin syntheses, selective formation of lighter olefins occurs due to the molecular sieving effect of the zeolite. However, when the reaction of the hydrocarbon occurs over acid sites located on the external surface of zeolite crystals, this results in a non-shape-selective reaction as well as coke deposition, leading to short lifetimes for the catalyst. These undesirable phenomena will be accelerated in nano-crystalline zeolites because of their large external surface areas. Accordingly, a method for selective deactivation of acid sites located on the external surface of zeolite crystals is desired in order to prevent these undesirable reactions. Masuda *et al.* (2001) have reported a method called the "catalytic cracking of silane method", in which SiO_2 units are formed selectively on the acid sites of the zeolite using organic silane compounds. Tago *et al.* (2009c) have reported that the yields of lighter olefins such as ethylene and propylene are increased over the selectively de-activated MFI zeolite.

3.2 Structured materials composed of zeolite nanocrystals

Since the nano-crystalline zeolites have large external surface areas, they are potential candidates for seed crystals from which a structured material can be prepared. Moreover, the micro- and meso-pores formed in nano-crystalline zeolites are characteristic of the structured materials. Accordingly, design of the micro- and meso-pores is important.
Serrano *et al.* have reported the preparation of micro-, meso-, and macroscopic hierarchical materials composed of nano-crystalline zeolites. They prepared hybrid zeolitic-mesoporous materials with the properties of both MCM-41 and MFI zeolite using zeolite seeds by assembling around cetyltrimetyl ammonium bromide micelles. Moreover, they have also developed other methods to fabricate hierarchical materials using organosilane bonded zeolite nanocrystals, where the degree of aggregation of the zeolite can be controlled.
Nano-crystalline zeolites have been used as seed crystals for zeolite membranes. Since the pore spaces and pore sizes in the crystals represent a very important factor, affecting membrane performances (Hasegawa *et al.*, 2007), nano-crystalline zeolite crystals are useful as seed crystals. In the preparation of zeolite membranes, after the deposition and/or seeding of the nano-crystalline zeolites on the base materials, secondary growth of the zeolite was carried out by a hydrothermal treatment (Kita *et al.*, 1995; Kondo *et al.*, 1997). Wang *et al.* (2002) have reported nano-structured zeolite 4A membranes, wherein nano-crystalline zeolites 4A were seeded on an alumina filter by a dip-coating method. Hasegawa *et al.* (2006) and Tago *et al.* (2008) have reported Silicalite-1 nanocrystal-layered membranes, where the Silicalite-1 nanocrystals are piled up on an alumina filter, followed by hydrothermal synthesis to form a Silicalite-1 layer on the nanocrystal layer. In these membranes, the thickness of the nanocrystal layer (amount of nano-crystalline zeolite used as seed crystals) can be easily changed, so that the separation properties of these membranes

can be controlled (Hedlund, *et al.*, 1999; Pera-Titus *et al.*, 2005). Moreover, because the zeolite crystals are seed crystals for the membranes, the separation properties of the membranes are improved with decreasing crystal sizes of the zeolite.

4. Conclusions

Zeolites are being used extensively in industrial processes such as heterogeneous catalysts and adsorbents. Nano-crystalline zeolites have large external surface areas as well as low diffusion resistance. Accordingly, control of the crystal size and the tailoring the mesopores and macropores among the crystals are important factors for applications of these nanocrystals. In order to obtain nano-crystalline zeolites, it is important to separate the nucleation and growth stages. The addition of a surfactant into synthetic solutions of zeolites is a promising method to control the crystal size and improve the crystallinity due to adsorption of the surfactant on the zeolite surface.

5. References

Aguadoa, J.; Serrano. D. P. & Rodriguez, J. M. (2008). *Micropor. Mesopor. Mat.*, 115, 3, 504-513, 1387-1811

Botella, P.; Corma, A., Iborra, S., Montón, R., Rodríguez, I. & Costa, V. (2007). *J. Catal.*, 250, 1, 161-170, 0021-9517

Burkett S.L. & Davis M.E. (1994). *J. Phys. Chem.*, 98, 17, 4647-4653, 0022-3654

Burkett S.L. & Davis M.E. (1995). *Chem. Matter.*, 7, 5, 920-928, 0897-4756

De Moor P. P. E. A.; Beelen T. P. M., Komanschek B. U., Beck L.W., Wagner P., Davis M. E. & Santen R. A. (1999a). *Chem. Eur. J.*, 5, 7, 2083-2088, 0947-6539

De Moor P. P. E. A.; Beelen T. P. M. & Van Santen, R. A. (1999b). *J. Phys. Chem. C.*, 103, 10, 1639-1650, 1089-5647

Dutta, P. K.; Rao, K. M. & Park, J. Y. (1991). *J. Phys. Chem.*, 95, 17, 6554-6656, 0022-3654

Grieken, R. V.; Sotelo, J. L., Menendez, J. M. & Melero, J. A. (2000). *Micropor. Mesopor. Mat.*, 39, 1-2, 135-147, 1387-1811

Groen, J. C.; Peffer, L. A. A., Moulijn, J. A. & Perez-Ramirez, J. (2004a). *Micropore. Mesopor. Mat.* 69, 1-2, 29-34, 1387-1811

Groen, J. C. ; Jansen, J. C., Moulijn, J. A. & Perez-Ramirez, J. (2004b). *J. Phys. Chem. B*, 108, 35, 13062-13065, 1520-6106

Hasegawa, Y.; Ikeda, T., Nagase, T., Kiyozumi, Y., Hanaoka, T. & Mizukami, F. (2006). *J. Membr. Sci.*, 280, 1-2, 397-405, 0376-7388

Hasegawa, Y.; Nagase, T., Kiyozumi, Y. & Mizukami, F. (2007). *J. Membr. Sci.*, 294, 1-2, 186-195, 0376-7388

Hedlund, J.; Noack, M., Kolsch, P., Creaser, D., Caro, J.& Sterte, J. (1999). *J. Membr. Sci.*, 159, 1-2, 263-273, 0376-7388

Hincapie, B. O. ; Garces, L. J., Zhang, Q., Sacco, A. & Suib, S. L. (2004). *Micropor. Mesopor. Mat.*, 67, 1, 19-26. 1387-1811

Jia, C. J.; Liu, Y., Schmidt, W., Lu, A. H. & Schuth, F. (2010). *J. Catal.*, 269, 1, 71-79, 0021-9517

Kita, H; Horii, K., Ohtoshi, Y., Tanaka, K. & Okamoto, K. (1995). *J. Mat. Sci. Lett.*, 14, 3, 206-208, 0261-8028

Kondo, M.; Komori, M., Kita, H. & Okamoto, K. (1997), *J. Membr. Sci.*, 133, 1, 133-141, 0376-7388
Kuechl, D. E.; Benin, A. I., Knight, L. M., Abrevaya, H., Wilson, S. T., Sinkler, W., Mezza, T. M. & Willis, R. R. (2010). *Micropor. Mesopor. Mat.*, 127, 1-2, 104-118, 1387-1811
Kumar, S.; Davis, T. M., Ramanan, H., Penn, R. L. & Tsapatsis, M. (2007). *J. Phys. Chem. B*, 111, 13, 3393-3403, 1520-6106
Larlus, O.; Mintova, S. & Bein, T. (2006). *Micropor. Mesopor. Mat.*, 96, 1-3, 405-412, 1387-1811
Larsen, S. C. (2007). *J. Phys. Chem. C*, 111, 50, 18464-18474, 1932-7447
Lee, S.; Carr, C. S. & Shantz, D. F. (2005). *Langmuir*, 21, 25, 12031-12036, 0743-7463
Li, Q. H.; Mihailova, B., Creaser, D. & Sterte, J. (2001). *Micropor. Mesopor. Mat.*, 43, 1, 51-59, 1387-1811
Li Q. H.; Mihailova, B., Creaser, D. & Sterte, J. (2000). *Micropor. Mesopor. Mat.*, 40, 1-3, 53-62, 1387-1811
Masuda, T.; Fukumoto, N., Kitamura, M., Mukai, S. R., Hashimoto, K., Tanaka, T. & Funabiki, T. (2001). *Micropor. Mesopor. Mat.*, 48, 1-3, 239-245, 1387-1811
Matsune, H.; Tago, T., Shibata, K., Wakabayashi, K. & Kishida, M. (2006). *J. Nanoparticle Research*, 8, 6, 1083-1087, 1388-0764
Mintova, S.; Olson, N. H., Valtchev, V. & Bein, T. (1999). *Science*, 283, 5405, 958-960, 0036-8075
Mintva, S. & Valtchev, V. (2002). *Micropor. Mesopor. Mat.* 55, 2, 171-179, 1387-1811
Mintova, S.; Valtchev, V., Onfroy, T., Marichal, C., Knozinger, H. & Bein, T. (2006). *Micropor. Mesopor. Mat.*, 90, 1-3, 237-245, 1387-1811
Morales-Pacheco, P.; Alvarez, F., Del Angel, P., Bucio, L. & Dominguez, J. M. (2007). *J. Phys. Chem. C*, 111, 6, 2368-2378, 1932-7447
Naik, S.P., Chen, J.C. & Chiang, A. S. T.(2002). *Micropor. Mesopor. Mat.*, 54, 3, 293-303, 1387-1811
Ogura, M.; Shinomiya, S., Tateno, J., Nara, Y., Nomura, M., Kikuchi, E. & Matsukata, M. (2001). *Appl. Catal. A. Gen.*, 219, 1-2, 33-43, 0926-860X
Pera-Titus, M.; Llorens, J., Cunill, F., Mallada, R. & Santamaria, J. (1995). *Catal. Today*, 104, 2-4, 281-287, 0920-5861
Ravishankar, R.; Kirschhock, C., Schoeman, B. J., Vanoppen, P., Grobet, P. J., Storck, S., Maier, W. F., Martens, J. A., DeSchryver, F. C. & Jacobs, P. A. (1998). *J. Phys. Chem. B*, 102, 15, 2633-2639, 1089-5647
Sakthivel, A.; Iida, A., Komura, K., Sugi, Y. & Chary K. V. R. (2009). *Micropor. Macropor. Mat.*, 119, 1-3, 322-330, 1387-1811
Serrano, D. P.; Aguado, J., Escola, J. M. & Rodriguez, J. M. (2005). *J. Anal. Appl. Pyrol.*, 74, 1-2, 353-360, 0165-2370
Serrano, D. P.; Aguado, J., Escola, J. M., Rodriguez, J. M. & Peral, A. (2006). *Chem. Mat.*, 18, 10, 2462-2464, 0897-4756
Serrano, D. P.; Garcia, R. A. & Otero, D. (2009). *Appl. Catal. A-Gen.*, 359, 1-2, 69-78, 0926-860X
Serrano, D. P.; Van Grieken, R., Melero, J. A., Garcia, A. & Vargas, C. (2010). *J. Mol. Catal. A: Chem.*, 318, 1-2, 68-74, 1381-1169
Song, W.; Justice, R. E., Jones, C. A., Grassian, V. H. & Larsen, S. C. (2004). *Langmuir*, 20 (2004) 4696
Song, W., Justice, R. E., Jones, C. A., Grassian, V. H. & Larsen, S. C., *Langmuir*, 20 (2004) 8301
Song, W.; Grassian, V. H. & Larsen, S. C. (2005). *Chem. Comm.*, 23, 2951-2953, 1359-7345

Tago, T.; Hatsuta, T., Miyajima, K., Kishida, M., Tashiro, S. & Wakabayashi, K. (2002). *J. Am. Ceram. Soc.*, 85, 9, 2188-2194, 0002-7820
Tago, T.; Tashiro, S., Hashimoto, Y., Wakabayashi, K. & Kishida, M. (2003). *J. Nanoparticle Research*, 5, 1-2, 55-60, 1388-0764
Tago, T.; Nishi, M., Kono, Y. & Masuda, T. (2004). *Chem. Lett.*, 33, 8, 1040-1041, 0366-7022
Tago, T.; Nakasaka, Y., Kayoda, A. & Masuda, T. (2008). *Micropor. Mesopor. Mat.*, 115, 1-2, 176-183, 1387-1811
Tago,T.; Iwakai,K., Nishi, N. & Masuda,T. (2009a). *J. Nanosci. Nanotechnol.*, 9, 1, 612-617, 1533-4880
Tago, T.; Aoki, D., Iwakai, K. & Masuda, T. (2009b). *Top. Catal.*, 52, 6-7, 865-871, 1022-5528
Tago, T.; Sakamoto, M., Iwakai, K., Nishihara, H., Mukai, S. R., Tanaka, T. & Masuda, T. (2009c). *J. Chem. Eng. Jpn.*, 42, 1, 162-167, 0021-9592
Takenaka, S.; Orita, Y., Matsune, H., Tanabe, E. & Kishida, M. (2007). *J. Phys. Chem. C*, 111, 21, 7748-7756, 1932-7447
Tosheva, L. & Valtchev, V. P. (2005). *Chem. Mater.*, 7, 10, 2494-2513, 0897-4756
Tsapatsis, M.; Lovallo, M. & Davis, M. E. (1996). *Micropor. Mat.*, 5, 6, 381-388, 0927-6513
Wang, H.; Huang, L., Holmberg B. A. & Yan, Y. (2002). *Chem. Comm.*, 16, 1708-1709, 1359-7345

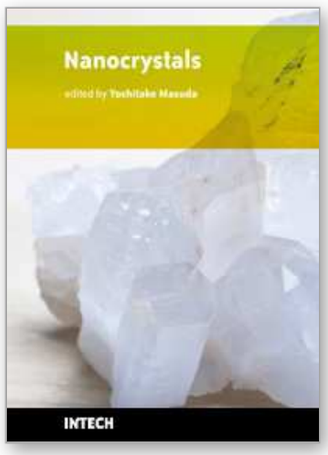

Nanocrystals

Edited by Yoshitake Masuda

ISBN 978-953-307-126-8
Hard cover, 326 pages
Publisher Sciyo
Published online 06, October, 2010
Published in print edition October, 2010

This book contains a number of latest research developments on nanocrystals. It is a promising new research area that has received a lot of attention in recent years. Here you will find interesting reports on cutting-edge science and technology related to synthesis, morphology control, self-assembly and application of nanocrystals. I hope that the book will lead to systematization of nanocrystal science, creation of new nanocrystal research field and further promotion of nanocrystal technology for the bright future of our children.

How to reference

In order to correctly reference this scholarly work, feel free to copy and paste the following:

Teruoki Tago and Takao Masuda (2010). Zeolite Nanocrystals- Synthesis and Applications, Nanocrystals, Yoshitake Masuda (Ed.), ISBN: 978-953-307-126-8, InTech, Available from: http://www.intechopen.com/books/nanocrystals/zeolite-nanocrystals-synthesis-and-applications

INTECH
open science | open minds

InTech Europe
University Campus STeP Ri
Slavka Krautzeka 83/A
51000 Rijeka, Croatia
Phone: +385 (51) 770 447
Fax: +385 (51) 686 166
www.intechopen.com

InTech China
Unit 405, Office Block, Hotel Equatorial Shanghai
No.65, Yan An Road (West), Shanghai, 200040, China
中国上海市延安西路65号上海国际贵都大饭店办公楼405单元
Phone: +86-21-62489820
Fax: +86-21-62489821

IntechOpen